Observation of correlated anti-Stokes emissions by multiwave mixing in sodium vapor

Koji Motomura
Japan Science and Technology Agency, 4-1-8 Honmachi, Kawaguchi 331-0012, Japan

Mayumi Tsukamoto, Akira Wakiyama, Ken-ichi Harada, and Masaharu Mitsunaga*
Graduate School of Science and Technology, Kumamoto University, Kumamoto 860-8555, Japan
(Received 8 December 2004; published 21 April 2005)

We study experimentally nonlinear optical processes in which Stokes and anti-Stokes fields build up under strong, resonant, counterpropagating pump laser excitation in atomic sodium vapor. We find that, at some pump frequency, two off-axis anti-Stokes emissions propagating along reflection-symmetric directions are strongly temporally correlated, with a correlation time of 0.5 μs and a correlation range of 1 mrad. It is shown by the numerical analysis based on six-wave mixing process involving pump, Stokes, and anti-Stokes waves in the forward and the backward directions that such correlated anti-Stokes emissions are possible when the medium is opaque for the Stokes field and transparent for the anti-Stokes field. Possibilities of quantum correlation for entangled photon generation using this system are discussed.

DOI: 10.1103/PhysRevA.71.043817 PACS number(s): 42.65.−k, 42.50.Gy, 42.50.Dv

I. INTRODUCTION

It has long been known that parametric processes due to strong nonlinear optical effects generate correlated emissions in different propagation directions satisfying the phase matching condition. Typical examples are found in parametric down conversion (three-wave mixing) in nonlinear crystals and nearly degenerate four-wave mixing in alkali atomic vapors [1]. In particular, correlated emissions, or twin photons, produced by parametric down converters (PDCs) are now essential ingredients of quantum information processing such as quantum cryptography and quantum teleportation [2]. In PDC, two waves, called signal and idler, are parametrically amplified under a strong, nonresonant pump beam excitation. Since they build up from a common infinitesimally small incident field, synchronization and correlation of the two emissions are guaranteed.

Correlated emissions in resonant systems like atomic vapors, on the other hand, have been less extensively studied, and applications to quantum communication have been few. Recently, using a Rb atomic vapor with a three-level Λ system, parametric self-oscillation was observed where Stokes and anti-Stokes photons are parametrically created by counterpropagating resonant excitation [3,4]. Besides, it was theoretically shown that generated Stokes and anti-Stokes photon pairs can be quantum-mechanically correlated [5]. An important advantage of using atomic vapors, compared to nonlinear crystals, is that generated emissions can be directly stored in their hyperfine splitting structure with a technique called light storage [6,7], or quantum memory [8–10], and can be retrieved at any time later, by applying a read pulse. In this way, both generation and storage of quantum information can be completed in the same sample with the same excitation wavelength in a compact experimental setup, and this very fact makes the study of correlated emissions in atomic vapors quite important and meaningful.

In this paper we will show our experimental studies of coherent emissions in a sodium (Na) atomic vapor by parametric processes. Two counterpropagating pump beams (forward and backward pumps) resonant to the Na D_1 transition are applied to the sample as illustrated in Fig. 1. Our experimental findings are summarized as follows: (1) Depending on the pump laser frequency, strong, coherent, off-axis (or conical) emissions are observed symmetrically in both the forward and the backward directions. (2) These conical emissions have distinct threshold behavior as a function of the pump intensity. This type of transverse pattern formation and threshold behavior has been reported earlier [11–13]. Temporal instabilities of these emissions have also been observed and analyzed extensively [14–17]. (3) These emissions are mainly composed of Stokes and anti-Stokes photons. (4) At one particular pump laser frequency, the emissions are almost purely anti-Stokes photons. (5) At this frequency, two anti-Stokes emissions, related by the reflection symmetry with respect to the plane perpendicular to the propagation axis (see Fig. 1), are strongly temporally correlated. In other words, the ones with wave vectors $\vec{k}_a$ and $\vec{k}_a - 2\vec{k}_p$ are correlated, where $\vec{k}_a$ and $\vec{k}_p$ denote wave vectors of anti-Stokes

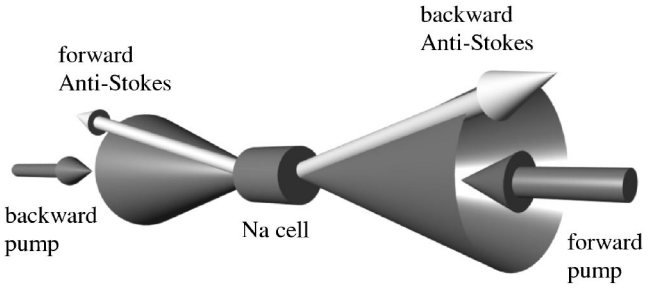

FIG. 1. Conical anti-Stokes emissions in the forward and the backward directions by the counterpropagating pump beams. Strongly correlated mirror-symmetric anti-Stokes emissions are indicated by arrows.

*Electronic address: mitunaga@sci.kumamoto-u.ac.jp

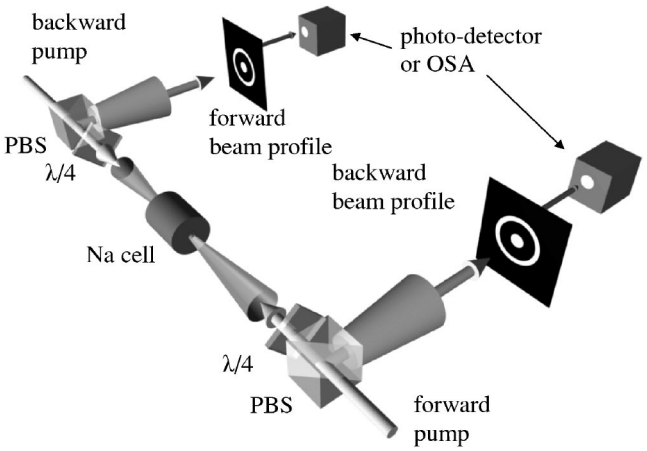

FIG. 2. Schematic of the experiment: (PBSs) polarizing beam splitters; (OSA) optical spectrum analyzer.

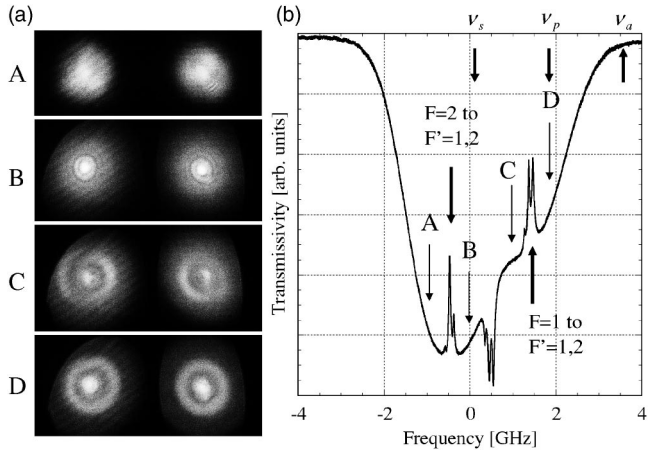

FIG. 3. (a) Photographs of forward and backward beam profiles at four different frequency positions, A, B, C, and D. (b) Saturated absorption spectrum of the $3S_{1/2}$-$3P_{1/2}$ D_1 transition of the Na atom, indicating the frequency positions A, B, C, and D. Stokes frequency ν_s and anti-Stokes frequency ν_a are also indicated when pump frequency ν_p is at D.

and pump beams. The last finding seems rather puzzling since we may think that two correlated emissions propagate point symmetrically ($\vec{k}_a$ and $-\vec{k}_a$) instead of mirror symmetrically. In order to explain this observation, we propose a six-wave mixing process where pump, Stokes, and anti-Stokes waves in the forward and the backward directions are involved, and we show by using a numerical simulation that, when there is a large difference between the absorption coefficients at the Stokes and the anti-Stokes frequencies, it is possible that two anti-Stokes emissions in the mirror symmetric directions are correlated. In the following sections we first explain our experimental setup and the experimental results, and then we present our interpretation of the observations.

II. EXPERIMENT

A. Setup

The experimental setup is schematically illustrated in Fig. 2. The basic configuration was similar to the ones shown in our previous works [18–20]. As a pump source, we employed a single-frequency ring dye laser (Coherent Radiation CR899-21), tuned around the $3S_{1/2}$-$3P_{1/2}$ D_1 transition of the Na atom at 589.6 nm. The beam, after passing through a Faraday isolator, was divided into two by a polarizing beam splitter (PBS) (not shown in Fig. 2) for the forward pump (FP) and the backward pump (BP) and the two beams (beam diameter, 2 mm) were impinged on a Na cylindrical cell (length 4.0 cm; diameter 2.5 cm) in a collinear, counterpropagating fashion as shown in Fig. 2. The peak linear transmission for a weak beam was almost null and the atomic density is estimated to be 3×10^{12} cm^{-3}. Typical powers of FP and BP in front of the cell were 40 mW, respectively. The Na cell did not contain any buffer gas and was surrounded by a magnetic shield. (We also tried a sample containing 30 Torr of Ne buffer gas, but the results reported below were not observed in this case.) Two quarter-wave plates placed on both sides of the cell allowed the transmitted FP and BP beams to reflect at the two PBSs, while maintaining the total symmetry with respect to forward and backward beams. The transmitted beams were analyzed in three ways. First of all, by placing paper cards, the beam profiles were checked by eyes or photographs. Second, a certain part of the beam pattern was sent through an iris (diameter 2 mm) and was received by an optical spectrum analyzer (OSA), with a free spectral range of 7.5 GHz, to check the optical spectrum of the emission. Third, the OSA was replaced by a photodetector followed by a digitizing oscilloscope for the analysis of temporal behavior of the emission. Great care was taken in the alignment to keep the symmetry for the backward and the forward directions.

B. Experimental results

As has been noted early, the onset and the behavior of the transverse pattern formation are very complicated, depending on many parameters such as pump intensity, pump frequency, and atomic density. As expected, the pump intensity dependence of these transverse patterns showed a clear threshold behavior, indicating that these emissions are due to parametric amplification and oscillation processes.

The pump frequency dependence of the transverse pattern was then studied. Basically, we observed off-axis, or conical emissions around the pump beam at four different frequency regions, A, B, C, and D as shown in Fig. 3(a). These frequency positions were identified by simultaneously taking the saturated absorption spectrum using a different Na cell, as shown in Fig. 3(b). Four points were located at a few hundred MHz to the lower side (A) and the higher side (B) of the $F=2$ to $F'=1,2$ hyperfine transitions and at a few hundred MHz to the lower side (C) and the higher side (D) of the $F=1$ to $F'=1,2$ hyperfine transitions. The transverse beam profile was sometimes very large and diffused (like point A), or sometimes very clear and distinct (like point D). In this paper, however, it is not our purpose to go into further detail on the frequency dependence of the beam profile. The ring patterns observed around the main pump beam were spec-

trally analyzed by using OSA, and it was found that they are composed mainly of the Stokes emission and the anti-Stokes emission and the ratio of those two intensities vary depending on the pump frequency.

The ring pattern was most clearly seen in the frequency region D, detuned 600 MHz to the high-frequency side of the $F=1$-$F'=2$ transition, and from now on, we will focus only on this pattern. This type of ring formation for the blue detuning is probabaly due to the positive nonlinear refractive index of the medium, as pointed out earlier [16]. A typical ring pattern is shown again in Fig. 4(a). The outer ring has a diameter of 18 mm and a width 2 mm at a distance 2 m away from the cell. The cone angle is thus 4.5 mrad. The intensity at the ring is 4.1 $\mathrm{mW/cm^2}$. By using an iris, we picked up one part of the ring and analyzed the spectrum by the OSA, and a typical OSA output is shown in Fig. 4(b). As it is clear, the emission is mainly anti-Stokes and the frequency ν_a is given by $\nu_a=\nu_p+\nu_{21}=\nu_p+1.772$ GHz, where ν_p is the pump frequency and ν_{21} is the hyperfine splitting frequency of the Na atom [15,16,21]. Although Stokes and pump components are slightly seen in Fig. 4(b) just for reference, they could become almost negligible with further alignment and we can assume that the emission is purely anti-Stokes. This spectrum was common for any part of the ring pattern. This may be reasonable because when ν_p is at frequency point D as shown in Fig. 3(b) ν_a is away from resonance and the absorption is negligible. On the other hand the Stokes frequency $\nu_s=\nu_p-1.772$ GHz is right at the center of the absorption and is subject to strong absorption. We will consider this problem in detail in Sec. III.

Next we analyzed the temporal behavior of anti-Stokes emissions by picking up certain points of the rings. In particular, we picked up two points denoted as α of the forward ring and point β of the backward ring [see Fig. 4(a)], corresponding to the emissions with the wave vectors related by reflection symmetry, i.e., $\vec{k}_a$ and $\vec{k}_a-2\vec{k}_p$. The results are shown in Fig. 4(c). The temporal wave forms of the signals were chaotic and no particular periodic components were found in the Fourier transform of this signal, but it is evident from this figure that the two wave forms have strong correlation. When these two wave forms are denoted as $f_\alpha(t)$ and $f_\beta(t)$, its cross-correlation function $g(\tau)$, given by

$$g(\tau)=\frac{\langle f_\alpha(t)f_\beta(t+\tau)\rangle}{\langle f_\alpha(t)\rangle\langle f_\beta(t+\tau)\rangle}, \tag{1}$$

can be calculated and presented in Fig. 4(d). The strong correlation peak at $\tau=0$ is seen with a correlation time $\tau_c=0.5$ μs.

This type of strong correlation is only seen when the two spots are chosen such that they are related by reflection symmetry and any other points show no correlation. Figure 5 shows the position dependence of the correlation functions. That is, in Fig. 4(a), with the spot α fixed, the spot β was moved by a distance $\delta=0,1,2,3$ mm away from the exactly correlated spot. This was done by moving the iris horizontally on the ring. The wave forms for these spots were taken and the corresponding cross-correlation functions are given in Fig. 5. This figure shows that the correlation takes place

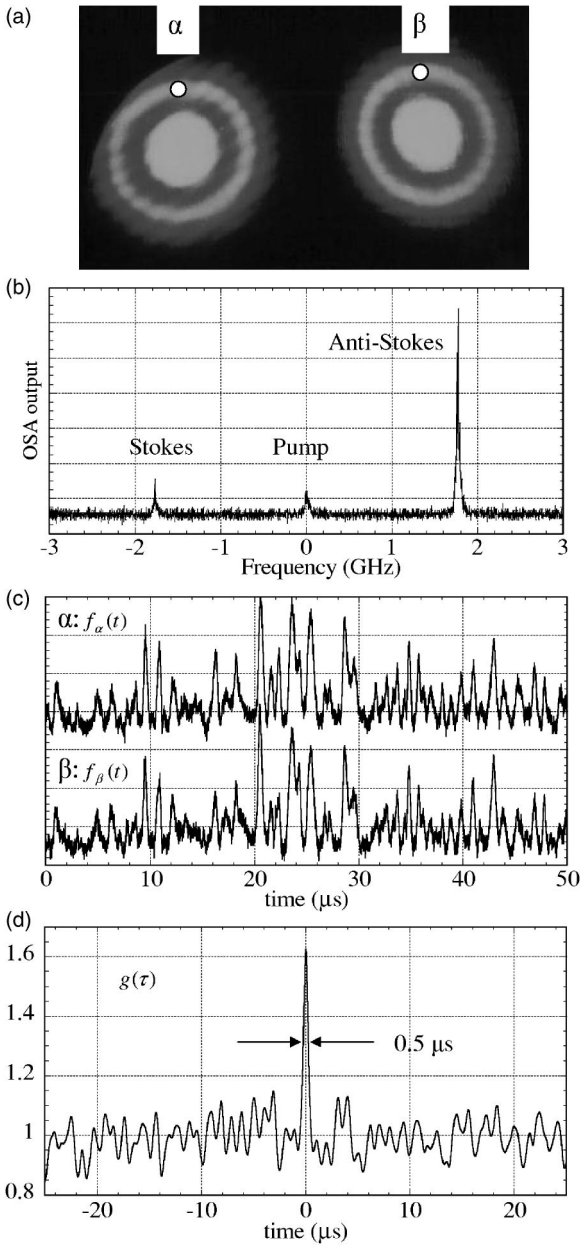

FIG. 4. (a) Forward and backward beam profiles when pump frequency was at D. Spots α and β in the rings indicate the parts where optical spectra and temporal wave forms were analyzed. (b) Optical spectrum analyzer (OSA) output of the spot α. A similar spectrum was obtained for the spot β. (c) Typical temporal wave forms for spot $\alpha[f_\alpha(t)]$ and spot $\beta[f_\beta(t)]$. (d) Cross-correlation of $f_\alpha(t)$ and $f_\beta(t)$ based upon Eq. (1).

only in the limited spatial range of $\sim$1 mm, or angle range of $\sim$1 mrad and, away from that, the emissions are regarded as totally independent. We have also tried correlation measurements for symmetrical points such as forward top versus forward bottom and forward top versus backward bottom. However, no apparent correlation was identified in these cases.

III. THEORY

From the experimental evidence, it is natural to conclude that two anti-Stokes emissions along $\vec{k}_a$ and $\vec{k}_a-2\vec{k}_p$ simulta-

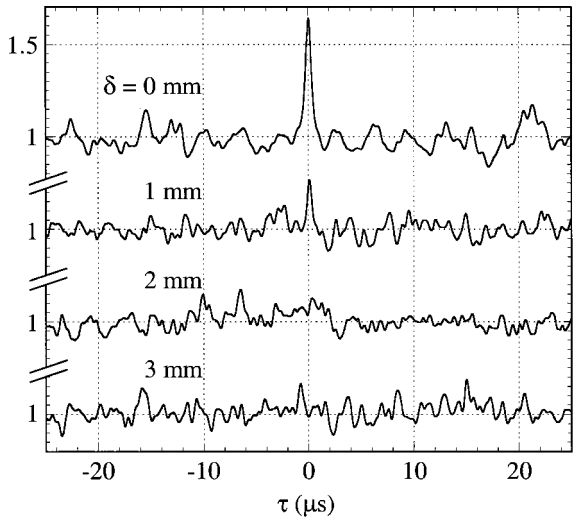

FIG. 5. Cross-correlation functions when the spot β was shifted by distances δ=0, 1, 2, and 3 mm, while the spot α was fixed.

neously and parametrically build up from the same infinitesimally small initial field (spontaneous emission), thus having strong temporal correlation. Our biggest concern was why it is so. It would have been more understandable if point-symmetric (counterpropagating) Stokes and anti-Stokes photons were correlated. The key to answer this problem seems to lie in the asymmetry in the absorption coefficients at the Stokes and anti-Stokes frequencies. As we mentioned in Sec. II and as it is shown in Fig. 3(b), when pump frequency ν_p is at position D, anti-Stokes frequency ν_a is in an almost transparent region while Stokes frequency ν_s is at the peak of the absorption spectrum. Therefore the Stokes field will experience strong attenuation while the anti-Stokes field will not. (Remember that, although the two-photon resonance condition $\nu_s=\nu_p-\nu_{21}$ is satisfied, electromagnetically induced transparency (EIT) does not take place when the pump fields are counterpropagating [22].)

To theoretically study this problem, in what follows we will consider a six-wave mixing process as shown in Fig. 6(a). The six waves include forward pump (wave vector $\vec{k}_p$), forward Stokes ($\vec{k}_s$), forward anti-Stokes ($\vec{k}_a$), backward pump ($-\vec{k}_p$), backward Stokes ($\vec{k}_s'$), and backward anti-Stokes ($\vec{k}_a'$). There are two kinds of four-wave mixing processes creating each Stokes or anti-Stokes photons. One is the forward scattering process [Fig. 6(b)] where two forward pump photons convert a forward Stokes to a forward anti-Stokes or vice versa. In this case, from momentum conservation, $\vec{k}_a=2\vec{k}_p-\vec{k}_s$. Similarly, two backward pump photons convert a backward Stokes to a backward anti-Stokes or vice versa ($\vec{k}_a'=-2\vec{k}_p-\vec{k}_s'$). The other process is the backward scattering process [Fig. 6(c)] where counterpropagating pump photons convert a forward Stokes to a backward anti-Stokes or vice versa ($\vec{k}_a'=-\vec{k}_s$ and $\vec{k}_s'=-\vec{k}_a$). By combining these two processes it is clear that the forward and the backward anti-Stokes beams are related as $\vec{k}_a'=\vec{k}_a-2\vec{k}_p$, i.e., mirror symmetric.

Now we start investigating the propagation of each field. We assume that the two pump fields are sufficiently strong

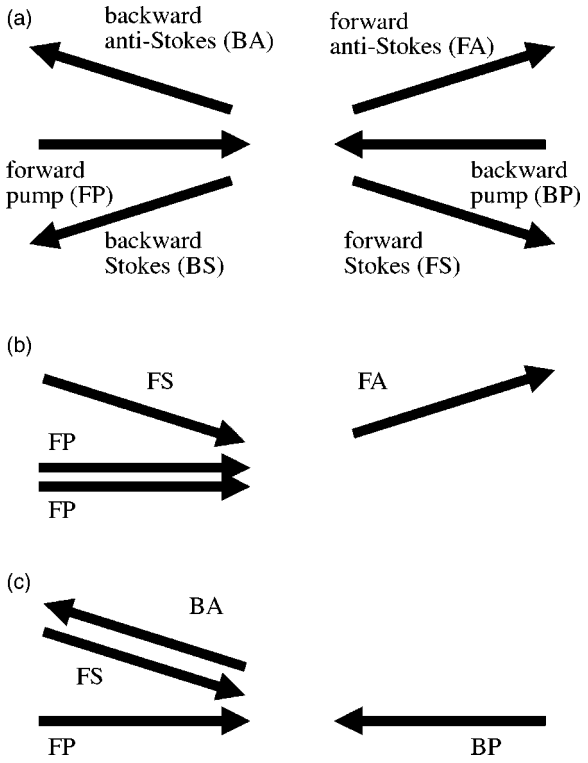

FIG. 6. (a) Six-wave mixing configuration where forward pump (FP), forward Stokes (FS), forward anti-Stokes (FA), backward pump (BP), backward Stokes (BS), and backward anti-Stokes (BA) are involved. (b) Forward scattering process where two FP photons and a FS photon generate a FA photon. (c) Backward scattering process where FP, BP, and FS photons generate a BA photon.

and the intensities are not affected by the other fields. Then we seek the propagations of the four light fields $\mathcal{E}_{fs}$, $\mathcal{E}_{fa}$, $\mathcal{E}_{bs}$, and $\mathcal{E}_{ba}$ corresponding to forward Stokes, forward anti-Stokes, backward Stokes, and backward anti-Stokes, respectively. Four macroscopic polarizations $\mathcal{P}_{fs}$, $\mathcal{P}_{fa}$, $\mathcal{P}_{bs}$, and $\mathcal{P}_{ba}$ should be basically derived by the three-level Liouville equations for four waves including the inhomogeneous Doppler broadening. To obtain the explicit forms of susceptibilities, detailed information of quantities such as optical and hyperfine-level dephasing times, pump Rabi frequencies, and the Doppler width is necessary [3,4,23]. Here, however, we will not try to derive the explicit forms, but will introduce these as parameters. By the symmetry consideration, there are only four susceptibilities, χ_f, χ_b, χ_s, and χ_a, and using these, the four polarizations are written as

$$\begin{aligned}
\mathcal{P}_{fs} &= \chi_f\mathcal{E}_{fa}^* + \chi_b\mathcal{E}_{ba}^* + \chi_s\mathcal{E}_{fs},\\
\mathcal{P}_{fa} &= \chi_f\mathcal{E}_{fs}^* + \chi_b\mathcal{E}_{bs}^* + \chi_a\mathcal{E}_{fa},\\
\mathcal{P}_{bs} &= \chi_f'\mathcal{E}_{ba}^* + \chi_b\mathcal{E}_{fa}^* + \chi_s\mathcal{E}_{bs},\\
\mathcal{P}_{ba} &= \chi_f'\mathcal{E}_{bs}^* + \chi_b\mathcal{E}_{fs}^* + \chi_a\mathcal{E}_{ba}.
\end{aligned} \tag{2}$$

The susceptibility χ_f (χ_f') is the one for the forward scattering process due to the forward (backward) pump beam and is proportional to the intensity of the forward (backward)

pump beam, while χ_b is the one for the backward scattering and is proportional to the product of the forward and backward pump amplitudes. The susceptibility χ_s (χ_a) describes the sum of the linear and nonlinear susceptibilities for the Stokes (anti-Stokes) field.

If these are substituted into Maxwell's propagation equations, we obtain the following equations:

$$\begin{aligned}
\frac{\partial \mathcal{E}_{fs}}{\partial z} &= -c_f \mathcal{E}_{fa}^* - c_b \mathcal{E}_{ba}^* - \frac{\alpha_s}{2}\mathcal{E}_{fs}, \\
\frac{\partial \mathcal{E}_{fa}}{\partial z} &= -c_f \mathcal{E}_{fs}^* - c_b \mathcal{E}_{bs}^* - \frac{\alpha_a}{2}\mathcal{E}_{fa}, \\
\frac{\partial \mathcal{E}_{bs}}{\partial z} &= c_f' \mathcal{E}_{ba}^* + c_b \mathcal{E}_{fa}^* + \frac{\alpha_s}{2}\mathcal{E}_{bs}, \\
\frac{\partial \mathcal{E}_{ba}}{\partial z} &= c_f' \mathcal{E}_{bs}^* + c_b \mathcal{E}_{fs}^* + \frac{\alpha_a}{2}\mathcal{E}_{ba},
\end{aligned} \tag{3}$$

where $c_f \equiv -(ik\chi_f/2\epsilon_0)$, $c_f' \equiv -(ik\chi_f'/2\epsilon_0)$, $c_b \equiv -(ik\chi_b/2\epsilon_0)$, $\alpha_s \equiv -(ik\chi_s/\epsilon_0)$, and $\alpha_a \equiv -(ik\chi_a/\epsilon_0)$ ($k \equiv |\vec{k}_s| \sim |\vec{k}_a|$). The above equations can be solved numerically, with a small amount of the initial field, say, forward Stokes. The boundary conditions at the sample ends at $z=0$ and L, then, are $\mathcal{E}_{fs}(0)=\mathcal{E}_0$, $\mathcal{E}_{fa}(0)=0$, $\mathcal{E}_{bs}(L)=0$, and $\mathcal{E}_{ba}(L)=0$.

The asymmetry between the Stokes and the anti-Stokes fields arises when the two absorption coefficients α_s and α_a differ by a large amount, in our case, $\alpha_s \gg \alpha_a$. Although the four quantities grow up owing to the coupling coefficients c_f, c_f', and c_b, only the anti-Stokes fields, free from absorpion, build up rapidly. Meanwhile the Stokes fields are attenuated by strong linear absorption. This situation becomes even more favorable for the anti-Stokes field if the optical pumping effect is taken into account. For the laser detuning to the high frequency side of resonance, the population is more accumulated to the $F=2$ hyperfine level than $F=1$, causing a stimulated Raman gain for the anti-Stokes field. In this case α_a can become even negative while α_s is still large. This argument is consistent with the fact that we have not observed conical anti-Stokes emissions in the sample with a buffer gas, where the optical pumping is not possible due to broad optical homogeneous linewidths.

An example of the numerical simulations for the above equations is shown in Fig. 7, and it shows that only the two anti-Stokes fields build up towards their propagation directions, starting from the common infinitesimally small initial field, thereby having a strong correlation. In the simulation we considered the simplest case where all χs appearing in Eq. (2) are purely imaginary, in which case all the quantities in Eq. (3) become real. (In the simulation, in order to suppress the divergence, the saturation factor $S=[1+(\mathcal{E}_{fs}^2+\mathcal{E}_{fa}^2+\mathcal{E}_{bs}^2+\mathcal{E}_{ba}^2)/\mathcal{E}_s^2]^{-1}$ was multiplied to c_f, c_f', and c_b ($\mathcal{E}_s$ is the saturation amplitude). The absorption of the pump field was also taken into account by adding the factor $\exp[-\alpha_p z]$ to c_f, and $\exp[-\alpha_p(L-z)]$ to c_f'. No factor is necessary for c_b because the two attenuations are cancelled out. The basic feature of the curves did not change for the case of negative α_a (stimulated Raman gain for the anti-Stokes field). It was also determined that the final curves do not change no matter which field was nonzero in the boundary conditions, and no matter how small the initial magnitude $\mathcal{E}_0$ is.

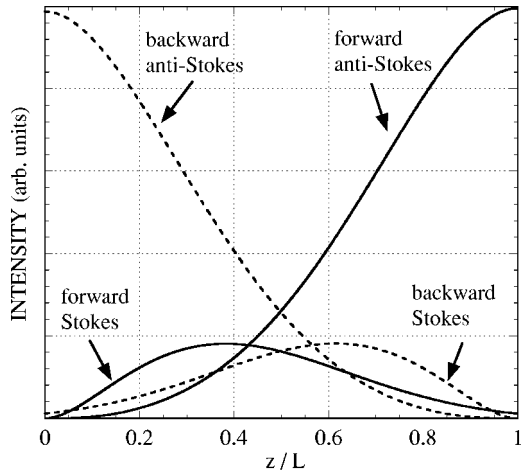

FIG. 7. Numerical simulation for the intensities of forward Stokes $\mathcal{E}_{fs}^2(z)$, forward anti-Stokes $\mathcal{E}_{fa}^2(z)$, backward Stokes $\mathcal{E}_{bs}^2(z)$, and backward anti-Stokes $\mathcal{E}_{ba}^2(z)$ waves as a function of the sample distance z. In the simulation, the parameters are set as $c_f=c_f'=c_b=5$, $\alpha_p=5$, $\alpha_s=10$, $\alpha_a=0.02$, $\mathcal{E}_s=8$, and $\mathcal{E}_0=0.01$.

IV. DISCUSSION AND CONCLUSION

In this paper we have limited ourselves to the case of classical correlations. It is no doubt, then, that it would be of great importance in the next stage to investigate quantum mechanical correlations between two anti-Stokes photons, either by taking fluctuation spectral density [9], or by obtaining correlation functions using a photon counting method and observing violation of a Cauchy-Schwarz inequality [10]. From the viewpoint of twin-photon generation, the discovery reported here has a couple of crucially important advantages. One is that they are off-axis emissions. The correlated photons reported so far in atomic vapors [9,10] have been on-axis emissions and in that case it is essential to spectrally filter out pump photons that are orders of magnitude larger in numbers than Stokes or anti-Stokes photons, which is a very challenging task [24]. In our case correlated photons are already spatially separated from pump photons and no spectral filtering is necessary. The other is that the off-axis emissions are purely anti-Stokes and we do not have to filter out Stokes emissions. Once correlated photon pairs are quantum mecahnically identified, it would be rather easy to generate entangled photon pairs. As a final goal, these entangled photon pairs will be stored and recalled at will in the atomic vapor cell by the quantum memory technique.

To summarize, parametric oscillations of Stokes and anti-Stokes fields by multiwave mixing under strong, resonant,

counterpropagating pump excitation in sodium atomic vapor have been studied. We found that two anti-Stokes emissions related by $\vec{k}_a$ and $\vec{k}_a - 2\vec{k}_p$ in wave vectors have strong temporal correlation, with a correlation time ~ 0.5 μs and a correlation range ~ 1 mrad. This seemingly peculiar correlation can be explained well by considering the six-wave mixing process with pump, Stokes, and anti-Stokes fields in both the forward and the backward directions. The extention of this study to investigate the existence of quantum correlation is definitely needed.

[1] M. O. Scully and M. S. Zubairy, *Quantum Optics* (Cambridge University Press, Cambridge, 1997).

[2] M. A. Nielsen and I. L. Chuang, *Quantum Computation and Quantum Information* (Cambridge University Press, Cambridge, 2000).

[3] M. D. Lukin, P. R. Hemmer, M. Löffler, and M. O. Scully, Phys. Rev. Lett. **81**, 2675 (1998).

[4] A. S. Zibrov, M. D. Lukin, and M. O. Scully, Phys. Rev. Lett. **83**, 4049 (1999).

[5] M. D. Lukin, A. B. Matsko, M. Fleischhauer, and M. O. Scully, Phys. Rev. Lett. **82**, 1847 (1999).

[6] C. Liu, Z. Dutton, C. H. Behroozi, and L. V. Hau, Nature (London) **409**, 490 (2001).

[7] D. F. Phillips, A. Fleischhauer, A. Mair, R. L. Walsworth, and M. D. Lukin, Phys. Rev. Lett. **86**, 783 (2001).

[8] M. Fleischhauer and M. D. Lukin, Phys. Rev. A **65**, 022314 (2002).

[9] C. H. van der Wal, M. D. Eisaman, A. André, R. L. Walsworth, D. F. Phillips, A. S. Zibrov, and M. D. Lukin, Science **301**, 196 (2003).

[10] A. Kuzmich, W. P. Bowen, A. D. Boozer, A. Boca, C. W. Chou, L.-M. Duan, and H. J. Kimble, Nature (London) **423**, 731 (2003).

[11] J. Pender and L. Hesselink, J. Opt. Soc. Am. B **7**, 1361 (1990).

[12] A. Petrossian, M. Pinard, A. Maître, J.-Y. Courtois, and G. Grynberg, Europhys. Lett. **18**, 689 (1992).

[13] R. S. Bennink, V. Wong, A. M. Marino, D. L. Aronstein, R. W. Boyd, C. R. Stroud, Jr., S. Lukishova, and D. J. Gauthier, Phys. Rev. Lett. **88**, 113901 (2002).

[14] A. L. Gaeta, R. W. Boyd, J. R. Ackerhalt, and P. W. Milonni, Phys. Rev. Lett. **58**, 2432 (1987).

[15] D. J. Gauthier, M. S. Malcuit, and R. W. Boyd, Phys. Rev. Lett. **61**, 1827 (1988).

[16] D. J. Gauthier, M. S. Malcuit, A. L. Gaeta, and R. W. Boyd, Phys. Rev. Lett. **64**, 1721 (1990).

[17] A. Maître, A. Petrossian, A. Blouin, M. Pinard, and G. Grynberg, Opt. Commun. **116**, 153 (1995).

[18] K. Motomura and M. Mitsunaga, J. Opt. Soc. Am. B **19**, 2456 (2002).

[19] H. Asahi, K. Motomura, K. Harada, and M. Mitsunaga, Opt. Lett. **28**, 1153 (2003).

[20] K. Motomura, T. Koshimizu, K. Harada, H. Ueno, and M. Mitsunaga, Opt. Lett. **29**, 1 (2004).

[21] V. Wong, R. S. Bennink, A. M. Marino, R. W. Boyd, C. R. Stroud, Jr., and F. A. Narducci, Phys. Rev. A **70**, 053811 (2004).

[22] M. Bajcsy, A. S. Zibrov, and M. D. Lukin, Nature (London) **426**, 638 (2003).

[23] M. D. Lukin, M. Fleischhauer, A. S. Zibrov, H. G. Robinson, V. L. Velichansky, L. Hollberg, and M. O. Scully, Phys. Rev. Lett. **79**, 2959 (1997).

[24] A. Heifetz, A. Agarwal, G. C. Cardoso, V. Gopal, P. Kumar, and M. S. Shahriar, Opt. Commun. **232**, 289 (2004).